Radio Frequency Electromagnetic Field Exposure of Insects at 10 cm from an Antenna

David Toribio, *Student Member, IEEE,* and Arno Thielens, *Member, IEEE*

***Abstract*—The increased exposure of insects to radio frequency electromagnetic fields (RF-EMFs) may have an impact on their health. The RF-EMF absorbed power in certain insects is considerably higher in the range of 6-300 GHz, due to more comparable wavelengths to their size. Likewise, in this range, the near-field interactions between antennas' and certain insects can significantly affect antennas' performance. Therefore, in this work, the volume and frequency dependencies of the RF-EMF absorbed power in various insects is evaluated in the range of 6-120 GHz, when placed at a fixed separation distance of 10 cm between the insects and the dipole antenna. Moreover, the effect of these insects on the dipoles' performance is assesed. To this aim, numerical simulations using finite-difference time-domain (FDTD) were performed on insect models obtained through micro-CT scanning. These simulation results showed an average absorbed power of $3.1 \pm 2.7\ \frac{mW}{W}$ at 6 GHz and of $3.4 \pm 2.8\ \frac{mW}{W}$ at 120 GHz. Additionally, they revealed that the absorbed power increases with increasing insect volume at an approximate rate of $2.5\ \frac{\mu W}{W \cdot mm^3}$ at 6 GHz, and of $1.2\ \frac{\mu W}{W \cdot mm^3}$ at 120 GHz, and that this rate of increase lowers with increasing frequency. Furthermore, results showed that the dipoles' gain pattern have a dependency on the insects' volume with a stronger dependency for higher frequencies.**

***Index Terms*—Radio frequency electromagnetic fields (RF-EMFs), RF-EMF exposure, insects, dipole antenna, millimeter waves.**

I. Introduction

Insects, which are essential for ecosystem functions like pollination, have been facing declining populations due to factors such as pesticides and habitat loss [1]. Given that 87% of food provisions from global food crop production depend on pollination [2], the ecological and economical importance of insects can't be understated. Therefore, studies investigating their decline have broadened to identifying additional factors and stressors that potentially affect insect health [3], such as their increasing exposure to radio-frequency electromagnetic fields (RF-EMFs) [4]–[6] caused by a growing demand for wireless telecommunication in society.

One of the changes in telecommunication networks, as they evolve from 2G to 5G, is the introduction of smaller carrier wavelengths (λ), comparable to the length of certain insects. Therefore, as shown in [9]–[12], the RF-EMF absorbed power in certain insects is frequency and size dependent and considerably higher in the range of 6-300 GHz.

In [12], the volume dependency of power absorption in insects was evaluated in the far field, and intriguinly, it was found that this power absorption strongly depends on insect volume. In [11], the frequency dependency of power absorption in a honey bee was evaluated in the near field of a dipole antenna in the range of 6-240 GHz. Due to the relatively small size of insects in comparison to the used carrier wavelengths in sub-6GHz telecommunication networks, near field interactions between insects and antennas have only been marginally studied [11]. However, in 5G networks, with higher carrier frequencies, these interactions have been shown to alter antennas' radiation efficiency, input impedance, and gain patterns, significantly, see [11], [13].

While [11] provided important results for bees near RF antennas, the question remains whether these results are representative for other insects. Therefore, the work presented in this manuscript aims to extend these results by evaluating the volume and frequency dependencies of the RF-EMF absorbed power in various insects in the frequency range of 6-120 GHz, in the vicinity of an emitting antenna. To this aim, this absorption is studied at a fixed separation distance between the insects and a dipole antenna of 10 cm, which can lay in the near or far field depending on the insect volume and the frequency studied. Moreover, the effect of the RF coupling between the antennas and the insects on the antennas' radiation performance is assessed.

These results are relevant for environmental policy makers that are tasked with protecting fauna and flora biodiversity. Moreover, they are also relevant for telecommunication companies that may need to take into account flying insects close to their antennas, such as companies providing Fixed Wireless Access services, which aim to provide internet to homes and businesses using mm-waves [14].

II. Methods

A. Studied insects

Table I shows the dimensions of the studied insects, which are the same models as studies in [10]–[12], [15]–[17], and their estimated resonance frequency range based on the longest diagonal of the smallest cube containing the insects ($Diag$), using the same prediction method as in [12]. According to this method, this range can be estimated by $\frac{c}{2 \cdot Diag} \leq f \leq \frac{2 \cdot c}{Diag}$, where c is the speed of light.

B. Numerical simulations

Numerical simulations were performed using the finite-difference time-domain (FDTD) method in Sim4Life (ZMT, Zurich, Switzerland) to estimate RF-EMFs in and around the insects. The spatial grid steps in the simulations were selected to be equal or lower to one tenth of the smallest wavelength

David Toribio and Arno Thielens are with the Department of Information Technology, Ghent Univerity-imec, 9052 Ghent, Belgium (e-mail: david.toribio@ugent.be).

Arno Thielens is also with the Advanced Science and Research Center of the Graduate Center of the City University of New York, New York, NY 10031, USA (email: athielens@gc.cuny.edu).

TABLE I
DIMENSIONS OF STUDIED INSECTS.

Insect	L (mm)	W (mm)	H (mm)	D (mm)	V (mm^3)	Estimated resonance range (GHz)
Female yellow fever mosquito	5.18	3.96	2.69	7.1	1.1	21.3 - 85
Male yellow fever mosquito	6.04	5.41	4.19	9.1	1.8	16.43 - 65.74
Granary weevil	4.44	2.39	2.19	5.5	3.2	27.29 - 109.14
Honeybee	11	4.23	3.66	12.3	54.6	12.1 - 48.7
Blue bottle fly	11.49	7.05	6.45	14.9	78.5	10.04 - 40.15
Sand wasp	19.62	15.50	10.56	27.1	242	5.53 - 22.11
Long horn beetle	23.68	23.36	12.63	35.6	340	4.33 - 16.86
Asian hornet	21.55	13.25	11.21	27.7	421.7	5.42 - 21.68
Eupholus beetle	41.63	30.18	16.15	53.9	1010	2.78 - 11.3
Black field cricket	45	23.49	15.67	53.1	1090	2.82 - 11.29
Christmas beetle	30.05	19.82	15.21	39.1	2430	3.84 - 15.35
Amycterine ground weevil	36.96	15.91	14.70	42.8	2520	3.5 - 14
Black palm weevil	41.15	19.83	15.80	48.3	2850	3.1 - 12.41
Jewel beetle	45.09	19.89	13.43	51.1	4150	2.94 - 11.75

in the simulation domain ($\frac{\lambda}{\sqrt{\epsilon_r}}$), as required by the FDTD algorithm to return stable solutions.

The dielectric properties of the insects were quantified as conductivity (σ) and relative permittivity (ϵ_r). The dielectric properties of the male and the female mosquito (ϵ_{r1} and σ_1) are the same used in [10]. The dielectric properties of the rest of the insects (ϵ_{r2} and σ_2) were assigned using the same literature database and interpolation used in [18]. The frequencies, grid steps, simulated periods and dielectric properties used in the simulations are shown in Table II.

TABLE II
SIMULATION SETTINGS AND DIELECTRIC PROPERTIES

	6 GHz	12 GHz	24 GHz	60 GHz	90 GHz	120 GHz
Maximal grid step (mm) / Simulated periods						
Female mosquito	0.56 / 9	0.32 / 11	0.19 / 16	0.09 / 38	0.06 / 45	0.1 / 55
Male mosquito	0.56 / 10	0.32 / 11	0.19 / 16	0.09 / 28	0.06 / 45	0.1 / 55
Granary weevil	0.05 / 9	0.23 / 11	0.16 / 15	0.09 / 37	0.06 / 44	0.1 / 54
Honeybee	0.4 / 9	0.23 / 11	0.16 / 15	0.09 / 28	0.07 / 45	0.1 / 55
Fly	0.4 / 10	0.23 / 12	0.16 / 16	0.09 / 28	0.1 / 48	0.1 / 59
Sand wasp	0.4 / 9	0.23 / 11	0.16 / 16	0.09 / 28	0.07 / 46	0.1 / 56
Long horn beetle	0.4 / 9	0.23 / 12	0.16 / 15	0.09 / 29	0.13 / 49	0.1 / 56
Hornet	0.4 / 9	0.23 / 11	0.16 / 16	0.09 / 28	0.13 / 46	0.1 / 56
Eupholus beetle	0.4 / 9	0.23 / 11	0.16 / 15	0.09 / 28	0.13 / 38	0.1 / 68
Black field cricket	0.4 / 10	0.23 / 12	0.16 / 16	0.09 / 29	0.13 / 50	0.1 / 60
Christmas beetle	0.4 / 9	0.23 / 11	0.16 / 16	0.09 / 60	0.13 / 40	0.1 / 60
Amycterine ground weevil	0.4 / 9	0.23 / 12	0.16 / 16	0.09 / 29	0.07 / 47	0.1 / 57
Black palm weevil	0.4 / 10	0.23 / 12	0.16 / 16	0.09 / 28	0.07 / 46	0.1 / 66
Jewel beetle	0.4 / 10	0.23 / 12	0.16 / 16	0.09 / 29	0.13 / 50	0.1 / 60
Dielectric properties						
ϵ_{r1}	19.6	15.1	10.7	6.8	5.7	5.3
σ_1 (S/m)	3.1	6.1	10.4	17.2	20.4	22.2
ϵ_{r2}	38	28.6	14.9	7	5.9	5.5
σ_2 (S/m)	5.1	12	21.1	27.9	28.9	29.2

The insects were modeled as homogeneous objects. For these simulations, half wavelength dipoles were designed to operate at the frequencies of interest and with a power reflection coefficient ($|S_{11}|^2$) lower than $-10\ dB$. The characteristics of these dipoles are the same as in [11].

For each frequency, one simulation was performed with each insect in the configuration presented in Fig. 1 with the separation distance (D) set to 10 cm. Therefore, the simulations' data set resulted in 6 (frequencies) + 14 (insects) = 98 simulations.

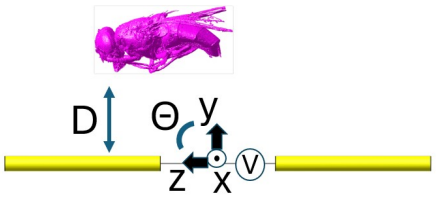

Figure 1: Orientations of the dipoles and the insects (shown here is the blue bottle fly). "D" is the separation distance between the dipole and the insects. "V" is the voltage source of the dipole. ϕ (not shown) is the angle between the x and y axes.

After each simulation, Sim4Life computes the internal electric field of the insects' model and uses it to calculate the whole-body absorbed RF-EMF power (P'_{abs}) in the insects. P'_{abs} is calculated as the integrated product of the conductivity and the squared internal electric field strength over the total volume (V) of the insect

$$P'_{abs} = \int_V \sigma \times |\vec{E_{int}}|^2 \ [W] \tag{1}$$

P'_{abs} is an important quantity since the dielectric heating of an insect is proportional to its absorbed RF-EMF power [19].

To validate the choice of grid step and simulation time, two simulations were run at 120 GHz with the Granary Weevil, where in one simulation the maximum grid step was set to 0.05 mm (half of the originally assigned, see Table II), and in the other simulation, the simulation time was set to 108 periods (double of the originally assigned).

Also, to validate the choice of dielectric properties, 4 simulations with the Granary Weevil, and 4 simulations with the female mosquito were performed at 24 GHz, in which their assigned dielectric properties (see Table II) were altered by: ($0.5 \cdot \epsilon_r$, $0.5 \cdot \sigma$), ($0.5 \cdot \epsilon_r$, $1.5 \cdot \sigma$), ($1.5 \cdot \epsilon_r$, $0.5 \cdot \sigma$), ($1.5 \cdot \epsilon_r$, $1.5 \cdot \sigma$). Then, after each simulation, the percentage change in P'_{abs} due to these alterations was computed.

C. Analysis of simulation results

In order to take into account the mismatch effect of the dipole due to the presence of each insect, P'_{abs} was normalized to the dipoles' accepted power. Moreover, to better compare the power absorption across the insects, this normalized absorbed power (P_{abs}) was normalized to the insects' volume (S_{abs}).

Additionally, in order to assess the internal P_{abs} distribution in the insects, the internal electric field intensities normalized to the maximum electric field intensity ($\frac{|\vec{E}|}{|\vec{E_{max}}|}$) in a slice in the YZ plane, at the center of each insect (x = 0 mm), were computed at each frequency.

Furthermore, to model P_{abs} as a function of volume (V) at each frequency, the following model was used [12]:

$$10 \cdot log_{10}\frac{P_{abs}}{1\,\frac{W}{W}} = a + b \cdot 10 \cdot log_{10}\frac{V}{1\,mm^3} + \chi(\mu, std) \quad (2)$$

where χ is a Gaussian distributed error term with mean (μ) and standard deviation (std).

Finally, to assess the precision of this model, its associated logarithmic root-mean-square error (RMSE) was computed according to the following equation:

$$RMSE = \sqrt{\frac{\sum_{i=1}^{n}(10 \cdot \log_{10}(P_{abs,i}) - 10 \cdot \log_{10}(\hat{P}_{abs,i}))^2}{n}} \quad (3)$$

where $P_{abs,i}$ is P_{abs} for insect (i), $\hat{P}_{abs,i}$ is the estimated P_{abs} of insect (i) according to the model in (2), and n is the number of insects studied.

III. Results and Discussion

A. Antenna parameters as a function of frequency

Fig. 2 shows that the maximum isotropic gain of the dipoles' radiation pattern when placed at 10 cm from an insect is higher than their theoretical free space gain of 2.15 dBi, and generally increases with frequency maximizing at 60 GHz or higher frequencies. Simulation results also showed that the radiation and mismatch efficiencies as a function of frequency only fluctuated slightly with a maximal deviation from their values at 6 GHz of 0.02% and 0.05%, respectively.

Fig. 3 shows that the gain pattern in the direction where the insects were located, $\phi = 90°$, has a dependency on the insect volume, showing larger deformations relative to the free space gain pattern for larger insects.

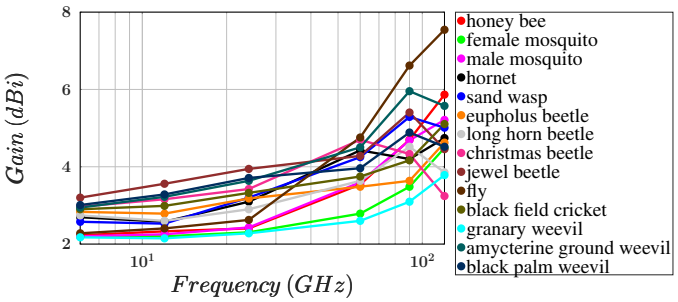

Figure 2: Maximum isotropic gain as a function of frequency.

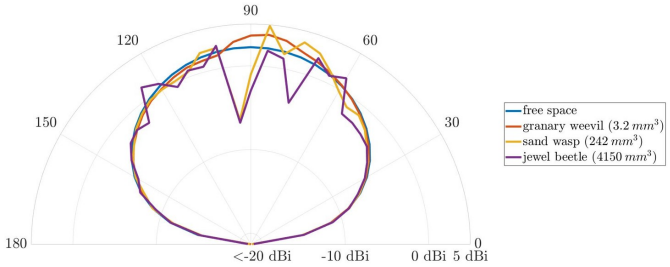

Figure 3: Gain as a function of θ, at $\phi = 90°$, at 120 GHz, in free space, for the Granary weevil, the Sand wasp and the Jewel Beetle.

B. Absorbed power as a function of frequency and insect volume

Fig. 4 shows a distribution of P_{abs} as a function of frequency with an average P_{abs} at 6 GHz of $3.1 \pm 2.7\ \frac{mW}{W}$, at 60 GHz of $3.7 \pm 3.2\ \frac{mW}{W}$, and at 120 GHz of $3.4 \pm 2.8\ \frac{mW}{W}$.

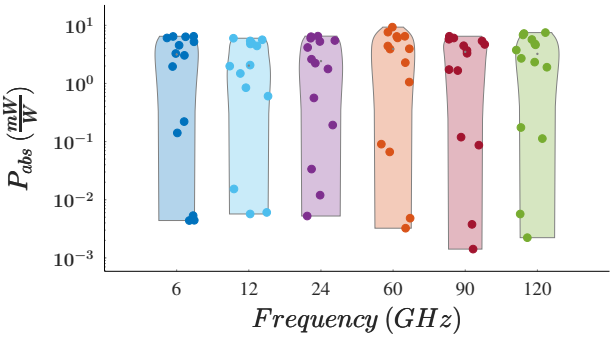

Figure 4: Absorbed power at D = 10 cm for an accepted power into the emitting dipole of 1 W.

Fig. 5 shows that as frequency increases from 6-120 GHz, S_{abs} for the honey bee, the fly, the male mosquito, and the granary weevil have relatively higher variations. This occurs because as shown in Table I, the estimated resonance frequency range of these smaller insects lies in the range from 6-120 GHz, and also because, when these insects are considered, 10 cm is in the far field region. This is in correspondence to the results presented in [9], [10], [12], where higher variations in P_{abs} near the resonance frequency of the insects were observed in the far field.

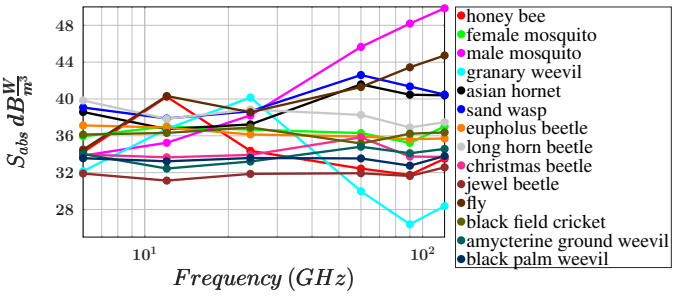

Figure 5: Absorbed power density at D = 10 cm relative to 1 (W/m^3) for an accepted power into the emitting dipole of 1 W.

Table III lists the parameter values of the model fit according to (2), and its associated RMSE according to (3). The values listed for a and b in Table III are the 95% confidence bounds of their fitted values.

TABLE III
MODEL FIT PARAMETERS

	6 GHz	12 GHz	24 GHz	60 GHz	90 GHz	120 GHz
a	(-58.33,-51.73)	(-54.65,-48.27)	(-53.13,-48.13)	(-57.06,-45.45)	(-58.66,-44.4)	(-56.61,-42.98)
b	(0.89,1.15)	(0.77,1.02)	(0.77,0.97)	(0.69,1.14)	(0.63,1.18)	(0.59,1.13)
RMSE	2.88	2.78	2.19	5.05	6.21	5.96

Fig. 6 shows that P_{abs} increases with increasing volume, at an approximate rate of 2.5 $\frac{\mu W}{mm^3}$ at 6 GHz, and of 1.2 $\frac{\mu W}{mm^3}$ at

120 GHz, for an accepted power into the emitting dipole of 1 W. In addition, it shows that the rate of increase of P_{abs} as a function of insect volume lowers with increasing frequency, when a and b are the upper and lower 95% confidence bounds of their fitted values, respectively, similar to the far field results obtained in [12]. This behavior is explained by the fact that the upper bound for a increases and the lower bound for b decreases as frequency increases, as shown in Table III.

Moreover, in Table III it is also seen that the RMSE is higher for higher frequencies. This occurs because the smaller insects resonate at higher frequencies, which leads to larger discrepancies in their S_{abs} (see Fig. 5), and thus higher variations in P_{abs} as a function of insect volume, at higher frequencies.

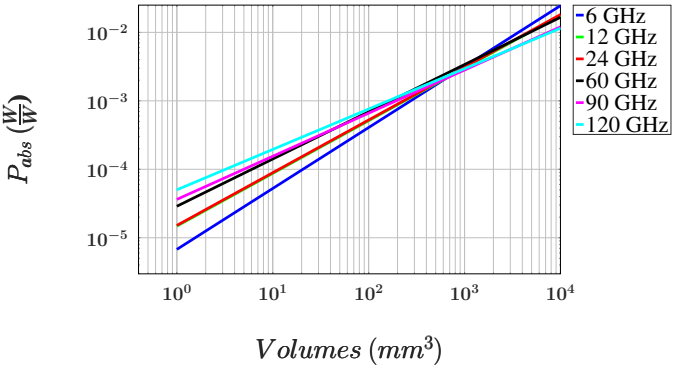

Figure 6: Absorbed power as a function of insect volume according to the fit of the simulation results to the model in (2).

.

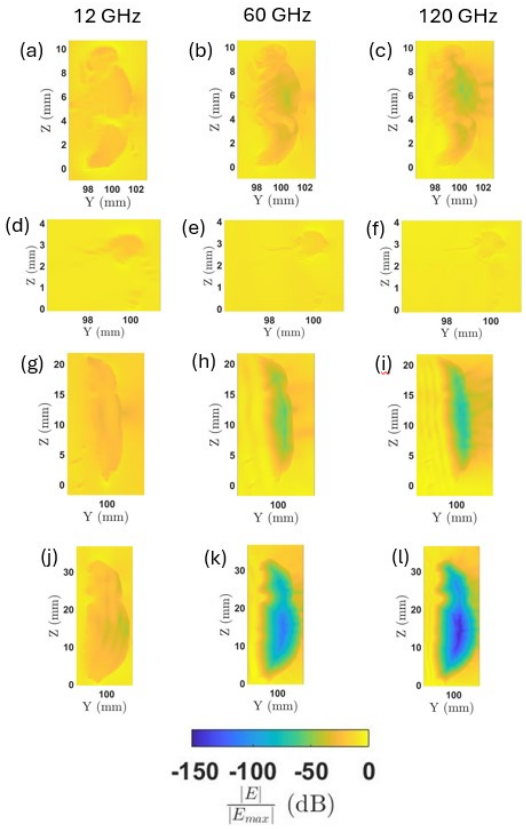

Figure 7: Internal electric field intensities. (a), (b), and (c) Fly. (d), (e), and (f) Male mosquito. (g), (h), and (i) Long horn beetle. (j), (k), and (l) Amycterine ground weevil

C. Insects' internal electric field

Simulation results also showed that internal $\frac{|\vec{E}|}{|\vec{E_{max}}|}$ in the insects experience a larger decay in those insects whose estimated resonance frequencies do not lie in the range of 6-120 GHz, which are also the larger insects (see Table I). As an example, Fig. 7 shows a larger decay of internal $\frac{|\vec{E}|}{|\vec{E_{max}}|}$ as a function of frequency in the amycterine ground weevil and the long horn beetle than in the fly and the male mosquito.

D. Uncertainties

The percentage change in P'_{abs} observed by altering the dielectric properties by $(0.5 \cdot \epsilon_r,\ 0.5 \cdot \sigma)$, $(0.5 \cdot \epsilon_r,\ 1.5 \cdot \sigma)$, $(1.5 \cdot \epsilon_r,\ 0.5 \cdot \sigma)$, $(1.5 \cdot \epsilon_r,\ 1.5 \cdot \sigma)$ with the Granary Weevil were: 27%, 36%, 47%, and 28%, respectively and with the female mosquito were: 31%, 61%, 54%, 28%, respectively. Moreover, the percentage change observed by reducing the maximum grid step by half was of 16%, and by doubling the simulation time was of 3%. These percentage changes are significant but are still much smaller than the change in P'_{abs} of more than a factor of 900 as a function of volume.

IV. Conclusion

Numerical simulations using FDTD were executed to calculate the whole-body absorbed radio frequency power P_{abs} of various insects at 10 cm from a dipole antenna, in the frequency range of 6-120 GHz. Simulation results showed an average P_{abs} at 6 GHz of $3.1 \pm 2.7\ \frac{mW}{W}$, and at 120 GHz of $3.4 \pm 2.8\ \frac{mW}{W}$. Additionally, they revealed that P_{abs} increases with increasing insect volume at an approximate rate of 2.5 $\frac{\mu W}{mm^3}$ at 6 GHz, and of 1.2 $\frac{\mu W}{mm^3}$ at 120 GHz, for an accepted power into the emitting dipole of 1 W. Moreover, it was found that the rate of increase of P_{abs} as a function of insect volume lowers with increasing frequency.

Additionally, results showed that S_{abs} for the smaller insects has a higher frequency dependency in the studied frequency range, and likewise, they showed that internal $\frac{|\vec{E}|}{|\vec{E_{max}}|}$ have a lower decay as a function of frequency in these insects. This is due to a stronger RF-EMF coupling into these insects.

Furthermore, a linear fit using the logarithm of P_{abs} and the logarithm of the insect volume was modeled at each frequency, with an RMSE of less than 7 dB, which is small in comparison to the variations in P_{abs} of more than 30 dB.

Moreover, results showed that the dipoles' gain pattern in the direction where the insects are located has a dependency on the insect volume with a stronger dependency for higher frequencies.

Future directions of this research will consist on assessing the RF-EMF interactions between heterogeneous insect models with tissue specific dielectric properties and phased arrays which are the antennas used in high frequency telecommunication networks.

ACKNOWLEDGMENT

This work was funded by the Research Foundation - Flanders (FWO) under grant agreement no. G033220N.

REFERENCES

[1] D. M. Katumo, H. Liang, A. C. Ochola, M. Lv, Q.-F. Wang, and C.-F. Yang, "Pollinator diversity benefits natural and agricultural ecosystems, environmental health, and human welfare," *Plant Diversity*, vol. 44, no. 5, pp. 429–435, 2022.

[2] A.-M. Klein, B. E. Vaissière, J. H. Cane, I. Steffan-Dewenter, S. A. Cunningham, C. Kremen, and T. Tscharntke, "Importance of pollinators in changing landscapes for world crops," *Proceedings of the royal society B: biological sciences*, vol. 274, no. 1608, pp. 303–313, 2007.

[3] P. H. T. F. (US), *Pollinator research action plan*. Pollinator Health Task Force, 2015.

[4] J. Wyszkowska, S. Shepherd, S. Sharkh, C. W. Jackson, and P. L. Newland, "Exposure to extremely low frequency electromagnetic fields alters the behaviour, physiology and stress protein levels of desert locusts," *Scientific reports*, vol. 6, no. 1, p. 36413, 2016.

[5] S. Shepherd, M. Lima, E. Oliveira, S. Sharkh, C. Jackson, and P. Newland, "Extremely low frequency electromagnetic fields impair the cognitive and motor abilities of honey bees," *Scientific reports*, vol. 8, no. 1, pp. 1–9, 2018.

[6] M. Treder, M. Müller, L. Fellner, K. Traynor, and P. Rosenkranz, "Defined exposure of honey bee colonies to simulated radiofrequency electromagnetic fields (rf-emf): Negative effects on the homing ability, but not on brood development or longevity," *Science of The Total Environment*, vol. 896, p. 165211, 2023.

[7] A. J. Vanbergen, S. G. Potts, A. Vian, E. P. Malkemper, J. Young, and T. Tscheulin, "Risk to pollinators from anthropogenic electro-magnetic radiation (emr): Evidence and knowledge gaps," *Science of the total environment*, vol. 695, p. 133833, 2019.

[8] D. Clarke, E. Morley, and D. Robert, "The bee, the flower, and the electric field: electric ecology and aerial electroreception," *Journal of Comparative Physiology A*, vol. 203, pp. 737–748, 2017.

[9] A. Thielens, M. K. Greco, L. Verloock, L. Martens, and W. Joseph, "Radio-frequency electromagnetic field exposure of western honey bees," *Scientific Reports*, vol. 10, no. 1, p. 461, 2020.

[10] E. De Borre, W. Joseph, R. Aminzadeh, P. Müller, M. N. Boone, I. Josipovic, S. Hashemizadeh, N. Kuster, S. Kühn, and A. Thielens, "Radio-frequency exposure of the yellow fever mosquito (a. aegypti) from 2 to 240 ghz," *PLOS Computational Biology*, vol. 17, no. 10, p. e1009460, 2021.

[11] D. Toribio, W. Joseph, and A. Thielens, "Near field radio frequency electromagnetic field exposure of a western honey bee," *IEEE Transactions on Antennas and Propagation*, vol. 70, no. 2, pp. 1320–1327, 2021.

[12] H. Herssens, D. Toribio, E. De Borre, and A. Thielens, "Whole-body averaged absorbed power in insects exposed to far-field radio frequency electromagnetic fields," *IEEE Transactions on Antennas and Propagation*, vol. 70, no. 11, pp. 11 070–11 078, 2022.

[13] D. Toribio and A. Thielens, "Design of an efficient antenna for asian hornet (vespa velutina) tracking using insect telemetry," in *2023 IEEE USNC-URSI Radio Science Meeting (Joint with AP-S Symposium)*. IEEE, 2023, pp. 73–74.

[14] K. Laraqui, S. Tombaz, A. Furuskär, B. Skubic, A. Nazari, and E. Trojer, "Fixed wireless access: On a massive scale with 5g," *Ericsson Technology Review*, vol. 94, no. 1, pp. 52–65, 2017.

[15] D. Bell, N. Bury, S. Gretton, N. Corps, D. Mortimore, and M. K. Greco, "An x-ray micro-computer tomography study of the malpighian tubules of the blue bottle blow fly (calliphora vomitoria) diptera: Calliphoridae," *Zoology*, vol. 149, p. 125972, 2021.

[16] T. Ijiri, H. Todo, A. Hirabayashi, K. Kohiyama, and Y. Dobashi, "Digitization of natural objects with micro ct and photographs," *Plos one*, vol. 13, no. 4, p. e0195852, 2018.

[17] C. V. Nguyen, D. R. Lovell, M. Adcock, and J. La Salle, "Capturing natural-colour 3d models of insects for species discovery and diagnostics," *PloS one*, vol. 9, no. 4, p. e94346, 2014.

[18] A. Thielens, D. Bell, D. B. Mortimore, M. K. Greco, L. Martens, and W. Joseph, "Exposure of insects to radio-frequency electromagnetic fields from 2 to 120 ghz," *Scientific Reports*, vol. 8, no. 1, p. 3924, 2018.

[19] I. C. on Non-Ionizing Radiation Protection *et al.*, "Guidelines for limiting exposure to electromagnetic fields (100 khz to 300 ghz)," *Health physics*, vol. 118, no. 5, pp. 483–524, 2020.